UNIVERSITY
OF TRENTO

DIPARTIMENTO DI INGEGNERIA E SCIENZA DELL'INFORMAZIONE

38123 Povo – Trento (Italy), Via Sommarive 14
http://www.disi.unitn.it

DUAL-BAND SPLINE-SHAPED PCB ANTENNA FOR WI-FI
APPLICATIONS

L. Lizzi, F. Viani, and A. Massa

January 2011

Technical Report # DISI-11-025

Dual-Band Spline-Shaped PCB Antenna for Wi-Fi Applications

Leonardo Lizzi, Federico Viani, and Andrea Massa

Abstract

In this letter, a dual-band PCB antenna suitable for Wi-Fi applications is described. The antenna geometry is modeled by means of a spline curve and a partial metallic ground plane. The proposed antenna is suitable for Wi-Fi bands and it guarantees good impedance matching conditions at the working frequencies centered at $2.448\,GHz$ and $5.512\,GHz$, respectively. A prototype of the synthesized antenna, built on an Arlon substrate, is analyzed to assess the effectiveness of the proposed antenna model in terms of VSWR values as well as radiation patterns.

Index Terms

PCB Antenna, Spline Shape, Wi-Fi Applications.

I. INTRODUCTION

In recent years, there has been a significant development of wireless communication systems for local area networks (WLANs). This has facilitated the connection and the data exchange between wireless devices, such as laptops, routers, PCs, and other portable wireless devices. For these applications, the Wireless Fidelity standard (Wi-Fi, IEEE 802.11 a/b/g/n) operating at 2.4 and 5 GHz is one of the most commonly used [1][2]. Therefore, there is a growing demand of radiating devices suitable for Wi-Fi applications. Such antennas must be able to guarantee suitable matching conditions in both Wi-Fi frequency bands. Moreover, to satisfy a standard constraint of today's communication devices, the antennas must be easily manufactured and integrated into system boards. Achieving these objectives is not a trivial task, especially when dealing with portable devices, since a high degree of miniaturization is usually required. Within such a framework, an effective solution is represented by printed circuit board (PCB) antennas, that not only meet the previous requirements, but also present other advantages such as low profile, cheap cost, light weight, robustness, and suitability for mass production.

As far as the multiband behavior is concerned, it is often obtained by properly modifying the reference geometry of a suitable radiation element. Examples of such a design procedure can be found in [3]-[8], where several multiband solutions based on the reference planar inverted-F antenna (PIFA) are described. However, it should be pointed out that excessive modifications and complex designs might strongly modify the original antenna impedance matching parameters (e.g., the $VSWR$ or the S_{11} scattering parameter) as well as the corresponding radiations indexes (e.g., the efficiency, the radiation patterns, and the polarization). Moreover, the architectural complexity of the radiator certainly causes an increase in the manufacturing costs [9].

Another promising approach to synthesize miniaturized and multiband radiators exploits the positive features of fractal shapes [10][11]. As a matter of fact, the self-similarity property of the fractal shapes is suitable to obtain a multifrequency resonances. However, classical fractal geometries usually present harmonic resonances instead of a multiband behavior [12]. In order to overcome such a drawback, a possible solution consists in perturbing the geometrical descriptors of the original fractal shape to allow an accurate tuning of the natural frequencies of the structure at hand [13][14]. However, the arising configurations might result in rather complex geometries characterized by high-resolution details quite difficult to be realized without very precise manufacturing procedures.

In this letter, a preliminary assessment of an approach based on spline shapes for multi-band systems is presented. More specifically, a dual-band spline-shaped prototype built on a PCB is described. Unlike other methods, the dual-band behavior is obtained by modifying a spline curve, which describes the antenna geometry. Such a simple description allows one to
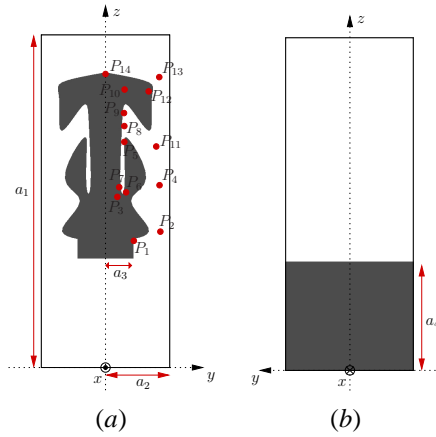
Fig. 1. Antenna geometry - (*a*) Front view and (*b*) back view.

generate in an easy fashion several candidate configurations aimed at satisfying both dimensional and electrical user-defined requirements. The result is a cheap and low profile PCB antenna suitable for integration and mass production, as well.

The rest of the paper is organized as follows. In Section II, the antenna geometry is described. Section III is aimed at presenting a selected set of numerical and experimental results illustrative of the performances of the synthesized prototype. Finally, some conclusions are drawn (Sect. IV).

II. ANTENNA DESIGN

Let us consider a microstrip structure printed on a planar dielectric substrate. Figure 1 shows the geometry of the proposed antenna model. It consists of a metallic patch and a partial ground plane, so that the antenna behaves like a monopole. The antenna presents a symmetry along the z-axis, so that only one half of the geometry is representative of the whole structure. On the front side of the dielectric substrate, the contour of the radiating part of the antenna is modeled by means of a cubic B-Spline curve, whose control points are denoted by $\{P_i = (y_i, z_i); i = 1, ..., 14\}$. The remaining part of the antenna structure is described by means of a set of geometrical variables $\{a_j; j = 1, ..., 4\}$. More in detail, a_1 and a_2 are the length and one half of the substrate width, respectively; a_3 is one half of the feedline width, and a_4 defines the length of the partial ground plane on the back of the antenna. Hence, the antenna geometry turns out to be uniquely identified by the values of the following descriptive parameters

$$\mathbf{s} = \{(y_i, z_i); i = 1, ..., 14; a_j; j = 1, ..., 4\} \tag{1}$$

under the assumption that the contour of the radiating element is a closed curve

$$\begin{cases} y_1 = a_3 \\ y_{14} = 0 \end{cases} \tag{2}$$

and that the feeding port is located at $P_F = (y_F = 0, z_F = a_4)$.

As far as the prototype at hand is concerned, the radiator has been required to operate in both Wi-Fi frequency bands from $f_{L1} = 2.412\,GHz$ up to $f_{H1} = 2.484\,GHz$ and from $f_{L2} = 5.150\,GHz$ up to $f_{H2} = 5.875\,GHz$, respectively. Moreover, to ensure good impedance matching conditions, a threshold value equal to $VSWR_{th} = 2$ has been imposed to the $VSWR$ over the operating bands. Concerning the geometrical constraints, the size of the antenna support has been limited to an area of $70 \times 70\,mm^2$. Then, the optimal shape of the antenna (i.e., $\mathbf{s}^{opt}$) has been determined by fitting the set of user-defined constraints and considering an iterative procedure [15] whose main blocks are an electromagnetic simulator based on the method-of-moment (MoM) [16] and a Particle Swarm Optimizer (PSO) [17]. Towards this end, the following cost function $\Psi(\mathbf{s})$ has been used

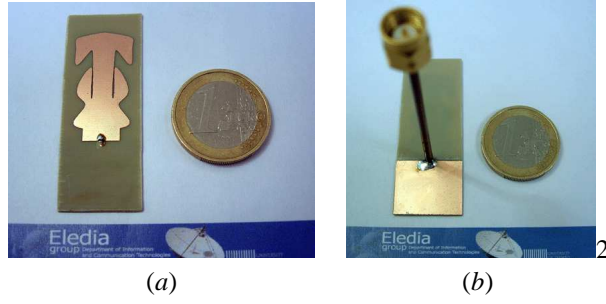$$\Psi(\mathbf{s}) = \Psi_1(\mathbf{s}) + \Psi_2(\mathbf{s}) + \Psi_{Rej}(\mathbf{s}) \tag{3}$$

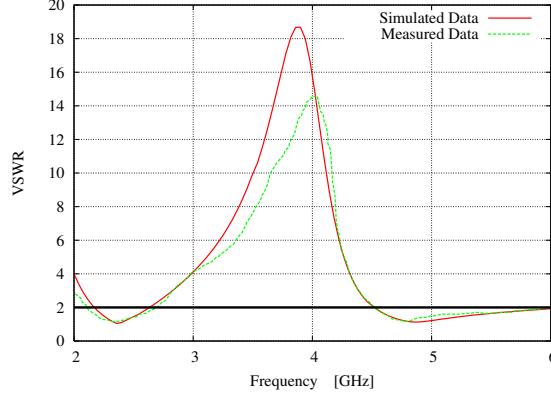Fig. 2. Antenna Prototype - (*a*) Front view and (*b*) back view.

Fig. 3. Simulated and measured VSWR values.

where

$$\Psi_1\left(\mathbf{s}\right) = \int_{f_{L1}}^{f_{H1}} \max\left\{0, \frac{VSWR\left(f\right) - VSWR_{th}}{VSWR_{th}}\right\} df \tag{4}$$

$$\Psi_2\left(\mathbf{s}\right) = \int_{f_{L2}}^{f_{H2}} \max\left\{0, \frac{VSWR\left(f\right) - VSWR_{th}}{VSWR_{th}}\right\} df \tag{5}$$

$$\Psi_{Rej}\left(\mathbf{s}\right) = \int_{f_{LR}}^{f_{HR}} \max\left\{0, \frac{VSWR_{Rej} - VSWR\left(f\right)}{VSWR_{Rej}}\right\} df. \tag{6}$$

More in detail, $\Psi_1\left(\mathbf{s}\right)$ and $\Psi_2\left(\mathbf{s}\right)$ are the terms concerned with the two $Wi-Fi$ bands, while $\Psi_{Rej}\left(\mathbf{s}\right)$ refers to the rejection band with the following parameter setting: $VSWR_{Rej} = 10$, $f_{LR} = 3.5\,GHz$, and $f_{HR} = 4.0\,GHz$ to force a true dual-band behavior.

After the optimization process, the geometric parameters of the prototype turned out to be: $a_1 = 50.1\,mm$, $a_2 = 9.6\,mm$, $a_3 = 4.2\,mm$, and $a_4 = 16.4\,mm$. Moreover, the coordinates of the spline control points resulted to be: $y_1 = 4.2\,mm$, $z_1 = 19.3\,mm$, $y_2 = 8.1\,mm$, $z_2 = 20.2\,mm$, $y_3 = 1.7\,mm$, $z_3 = 25.7\,mm$, $y_4 = 8.0\,mm$, $z_4 = 27.2\,mm$, $y_5 = 2.7\,mm$, $z_5 = 36.0\,mm$, $y_6 = 2.8\,mm$, $z_6 = 33.6\,mm$, $y_7 = 3.0\,mm$, $z_7 = 25.7\,mm$, $y_8 = 1.9\,mm$, $z_8 = 25.7\,mm$, $y_9 = 2.6\,mm$, $z_9 = 37.8\,mm$, $y_{10} = 2.6\,mm$, $z_{10} = 41.3\,mm$, $y_{11} = 7.5\,mm$, $z_{11} = 32.7\,mm$, $y_{12} = 6.4\,mm$, $z_{12} = 41.2\,mm$, $y_{13} = 8.1\,mm$, $z_{13} = 43.0\,mm$, $y_{14} = 0.0\,mm$, and $z_{14} = 44.3\,mm$. As it can be verified, the synthesized solution fits the size requirement being characterized by an overall dimension of $50.2 \times 19.2\,mm^2$.

III. NUMERICAL AND EXPERIMENTAL VALIDATION

The performance of the dual-band spline-shaped antenna has been numerically and experimentally evaluated. Towards this end, a prototype of the synthesized antenna (Fig. 2) has been printed with a photo-lithographic process on an Arlon dielectric substrate ($\varepsilon_r = 3.38$) of $0.78\,mm$ thickness. The prototype has been equipped with a SMA connector and fed by a coaxial
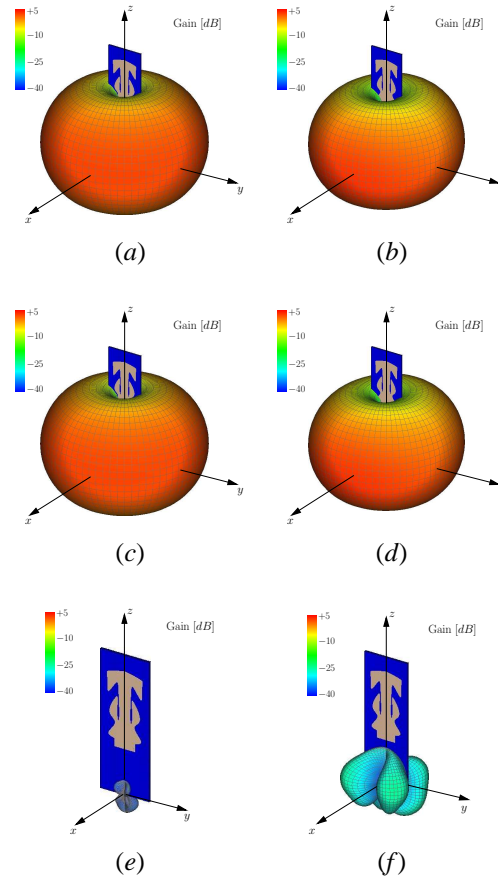
Fig. 4. Simulated 3D radiation patterns - Total gain at (a) $f_1 = 2.448\,GHz$ and (b) $f_2 = 5.512\,GHz$. Co-polar component at (c) $f_1 = 2.448\,GHz$ and (d) $f_2 = 5.512\,GHz$. Cross-polar component at (e) $f_1 = 2.448\,GHz$ and (f) $f_2 = 5.512\,GHz$.

cable in order to measure its electrical parameters.

As far as the impedance matching is concerned, Figure 3 shows a comparison between simulated and measured VSWR values. As it can be noticed, there is a good agreement between measured and simulated values over the entire frequency range. Moreover, the obtained results confirm that the antenna design as well as the corresponding prototype fit the project guidelines showing a VSWR lower than 2 in both the Wi-Fi operating bands. The measured bandwidths turn out to be quite large. The former is equal to $500\,MHz$, from 2.1 up to $2.6\,GHz$, and a fractional bandwidth equal to 21%. The second one is equal to $1.5\,GHz$, from 4.5 up to $6\,GHz$, with a fractional bandwidth of 29%. Such a wideband behavior is due to the spline shape that already demonstrated, as other planar monopole shapes, its effectiveness and reliability in designing wideband and ultra-wideband antennas [15]. As regards to the radiation properties of the prototype, the three-dimensional radiation patterns of the device under test are displayed in Fig. 4. Each diagram refers to the central frequency of a $Wi-Fi$ working band (i.e., $f_1 = 2.448\,GHz$ and $f_2 = 5.512\,GHz$). As expected, the antenna behaves as a dipolar radiator at both the working frequencies [Figs. 4(a)-(b)], showing an omnidirectional radiation pattern on the horizontal plane. Moreover, it can be observed that no additional lobes appear in the radiation patterns at the higher frequency band confirming the multi-band behavior of the antenna. As a matter of fact, the presence of additional lobes would indicate that the current mode at the $5\,GHz$ band is a simple overtone of the fundamental mode in the 2.4 GHz band, analogous to what occurs at higher frequencies with a wire monopole or a dipole antenna. For completeness, the co-polar components [Figs. 4(c)-4(d)] and the cross-polar ones [Figs. 4(e)-4(f)] are shown, as well. As it can be observed, the cross-polar components turn out to be smaller than the co-polar ones and the corresponding maximum gain values are equal to $-34\,dB$ (vs. $2\,dB$) and $-24\,dB$ (vs. $3\,dB$) at $2.4\,GHz$ and $5\,GHz$, respectively. In order to further assess and experimentally validate these indications on the radiation features of the antenna model, a set of measurements has been carried out by probing the synthesized prototype in a controlled measurement environment. The obtained results are shown in Fig. 5. Once again, there is a good agreement between simulated and measured
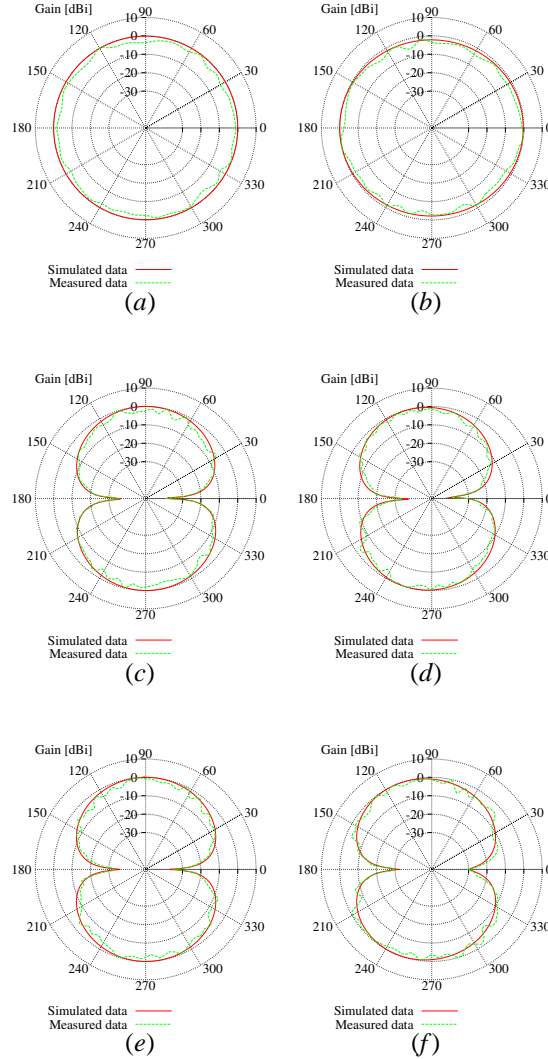
Fig. 5. Simulated and measured radiation patterns - Horizontal plane ($\theta = 90°$) at (a) $f_1 = 2.448\,GHz$ and (b) $f_2 = 5.512\,GHz$. Vertical plane ($\phi = 0°$) at (c) $f_1 = 2.448\,GHz$ and (d) $f_2 = 5.512\,GHz$. Vertical plane ($\phi = 90°$) at (e) $f_1 = 2.448\,GHz$ and (f) $f_2 = 5.512\,GHz$.

values. The measured patterns confirm the omnidirectional behavior of the antenna in the horizontal plane [$\theta = 90°$ - Figs. 5(a)-5(b)] as well as the presence of the nulls of the radiation diagrams along the z-direction [$\phi = 0°$ - Figs. 5(c)-5(d); $\phi = 90°$ - Figs. 5(e)-5(f)].

Finally, for completeness, Figure 6 gives a pictorial representation of the currents flowing on the metallic surfaces of the antenna geometry. More specifically, the amplitudes of the surface currents computed at f_1 and f_2 are displayed. As expected, the concentration of the current shifts to different portions of the antennas in the two different operating bands further confirming the true dual-band behavior of the antenna.

IV. CONCLUSIONS

In this letter, a dual-band spline-shaped PCB antenna suitable for Wi-Fi applications has been described. The antenna has been synthesized to achieve a good impedance matching in both the 2.4 and 5 GHz Wi-Fi bands. A prototype of the synthesized antenna has been built on a dielectric substrate. The effectiveness and reliability of the antenna model as well as the corresponding prototype has been assessed by means of numerical simulations and experimental measurements of both electrical and radiation parameters.
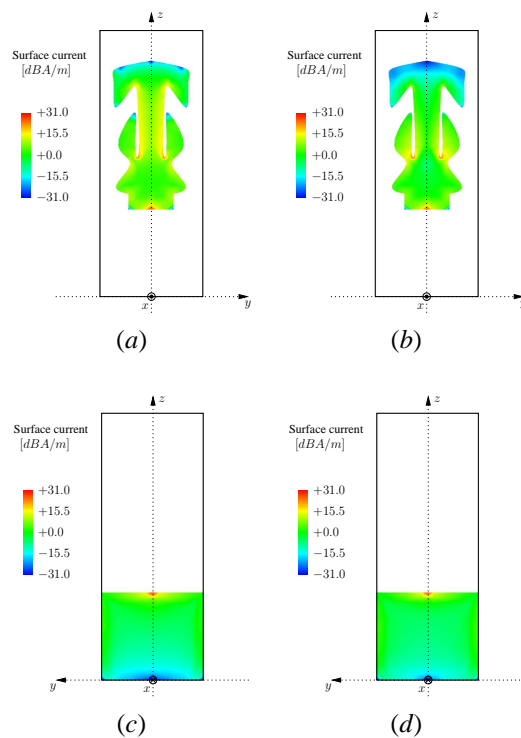
Fig. 6. Simulated surface current - Front view at (*a*) $f_1 = 2.448\,GHz$ and (*b*) $f_2 = 5.512\,GHz$. Back view at (*c*) $f_1 = 2.448\,GHz$ and (*d*) $f_2 = 5.512\,GHz$.

REFERENCES

[1] X. N. Low, W. K. Toh, and Z. N. Chen, "Broadband suspended plate antenna for WiFi/WiMAX applications," in *6th Int. Conf. Commun. Signal Process.*,2007, pp. 1-5.

[2] Y. Shen, Y. Wang, and S. Chung, "A printed triple-band antenna for WiFi and WiMAX applications," in *Asia Pacific Microwave Conf.*, 2006, pp. 1715-1717.

[3] O. Saraereh, M. Jayawardene, P. McEvoy, and J. C. Vardaxoglou, "Quad-band handset antenna operation for GSM900/DCS1800/PCS1900/UMTS," in *IEE Wideband Multi-band Antennas Arrays*, 2005, pp. 129-133.

[4] C. Di Nallo and A. Faraone, "Multiband internal antenna for mobile phones," *Electron. Lett.*, vol. 41, no. 9, pp. 514-515, Apr. 2005.

[5] Y. X. Guo, M. Y. W. Chia, and Z. N. Chen, "Miniature built-in quad-band antennas for mobile handsets," *IEEE Antennas Wireless Propagat. Lett.*, vol. 2, pp. 30-32, 2003.

[6] F.-R. Hsiao and K.-L. Wong, "Compact planar inverted-F patch antenna for triple-frequency operation," *Microw. Opt. Techn. Lett.*, vol. 33, no. 6, pp. 459-462, 2002.

[7] Y.-S. Wang, M.-C. Lee, and S.-J. Chung, "Two PIFA-related miniaturized dual-band antennas," *IEEE Trans. Antennas Propagat.*, vol. 55, no. 3, pp. 805-811, 2007.

[8] D.-Y. Kim, J. W. Lee, C. S. Cho, and T. K. Lee, "Design of a compact tri-band PIFA based on independent control of the resonant frequencies," *IEEE Trans. Antennas Propagat.*, vol. 56, no. 5, pp. 1428-1436, 2008.

[9] J. S. Lee, H. Rhyu, and B. Lee, "Design concept of multi-band antenna with resonant circuit on PCB," *Electron. Lett.*, vol. 43, no. 6, pp. 5-6, Mar. 2007.

[10] D. H. Werner and R. Mittra, *Frontiers in Electromagnetics*. Piscataway, NJ: IEEE Press, 2000.

[11] J. Gianvittorio and Y. Rahmat-Samii, "Fractal antennas: a novel antenna miniaturization technique, and applications," *IEEE Antennas Propagat. Mag.*, vol. 44, no. 1, pp. 20-36, Feb. 2002.

[12] C. P. Baliarda, J. Romeu, and A. Cardama, "The Koch monopole: a small fractal antenna," *IEEE Antennas Propag. Mag.*, vol. 48, no. 11, pp. 1773-1781, Nov. 2000.

[13] C. Puente, J. Romeu, R. Bartolome, and R. Pocus, "Perturbation of the Sierpinski antenna to allocate operating bands," *Electron. Lett.*, vol. 32, no. 24, pp. 1-2, Nov. 1996.

[14] R. Azaro, F. De Natale, M. Donelli, E. Zeni, and A. Massa, "Synthesis of a prefractal dual-band monopolar antenna for GPS applications," *IEEE Antennas Wireless Propag. Lett.*, vol. 5, no. 1, pp. 361-364, Dec. 2006.

[15] L. Lizzi, F. Viani, R. Azaro, and A. Massa, "Optimization of a spline-shaped UWB antenna by PSO," *IEEE Antennas Wireless Propag. Lett.*, vol. 6, pp. 182-185, 2007.

[16] R. F. Harrington, *Field Computation by Moment Methods*. Malabar, FL: Robert E. Krieger Publishing Co., 1987.

[17] J. Robinson and Y. Rahmat-Samii, "Particle swarm optimization in electromagnetics," *IEEE Trans. Antennas Propag.*, vol. 52, no. 2, pp. 397-407, Feb. 2004.